Supporting Information

Two-Dimensional Mercury(II)–Acetylide Framework with Built-in Dipole Field for Efficient Photocatalytic CO_2-to-CO Conversion

Mude Zhu,[a,c] Muchun Xu,[a] Lincan Fang,[*b] Linli Xu[*a,c]

[a]Department of Applied Biology and Chemical Technology and Research Institute for Smart Energy, The Hong Kong Polytechnic University (PolyU), Hung Hom, Kowloon, Hong Kong SAR, P. R. China.

[b]Key Laboratory of Functional Molecular Solids Ministry of Education, College of Chemistry and Materials Science, Anhui Normal University, Wuhu, Anhui, 241002, P. R. China.

[c]PolyU Shenzhen Research Institute, Shenzhen, 518057, P. R. China.

Contents

1. General Information

1.1 Chemicals

All reagents were obtained from commercial suppliers and used as received without further purification. 2,7,10,15-Tetrakis((trimethylsilyl)ethynyl)dibenzo[g,p]chrysene (TTED-TMS) was purchased from Yanshen (Extension) Technology Corporation Limited. Copper(I) iodide (CuI) was supplied by J&K. Mercury(II) chloride ($HgCl_2$) was provided by Macklin. Anhydrous chlorobenzene (99.5%) and tetrahydrofuran (THF, 99.5%) were obtained from Energy Chemical. Methanol (CH_3OH, ACS grade), acetonitrile (CH_3CN, ACS grade), and THF (ACS grade) were purchased from Damas-Beta. Tetrabutylammonium fluoride (TBAF, 1.0 M in THF) were obtained from Sigma Aldrich.

1.2 Synthesis of TTED

The trimethylsilyl protecting groups of TTED-TMS were deprotected using a TBAF solution to yield 2,7,10,15-tetrakis(ethynyl)dibenzo[g,p]chrysene (TTED). ^{1}H NMR (600 MHz, Chloroform-*d*) δ: 3.76 – 3.70 (m, 2H), 2.18 (s, 1H), 1.25 (t, J = 7.0 Hz, 4H). ^{13}C NMR (151 MHz, Chloroform-*d*) δ: 58.51, 18.45. MALDI-TOF: $[M+H]^+$ = 425.13, found = 424.96.

1.3 PFM and KPFM Measurements

Powdered TTED-Hg-AF samples were dispersed in ethanol by ultrasonication for 5 minutes. A 60 μL aliquot of the suspension was drop-cast onto a 1 × 1 cm^2 indium-tin -oxide (ITO) substrate and electrically connected to an iron plate using conductive silver paste. Piezoelectric amplitude and phase mapping were recorded using a Bruker Multimode 8 atomic force microscope (AFM) operating in piezoresponse force microscopy (PFM) mode. Kelvin probe force microscopy (KPFM) measurements were performed in electromagnetic mode using Pt/Ir-coated AFM tips.

1.4 Electrochemical Measurements

For Mott-Schottky (M−S) and electrochemical impedance spectroscopy (EIS) analyses, the working electrodes were prepared as follows: 1.0 mg of catalyst was dispersed in a mixture of 0.75 mL H_2O, 0.25 mL isopropyl alcohol, and 0.03 mL Nafion solution, followed by ultrasonication for 10 min. The resulting suspension was drop-cast onto a 1 × 1 cm^2 ITO plate and dried to form a uniform film.

All electrochemical measurements, including piezoelectric current tests, EIS, and M–S analyses, were carried out using a CHI660E electrochemical workstation. A typical three-electrode system was employed, consisting of the sample-coated electrode as the working electrode, a platinum wire as the counter electrode, and an Ag/AgCl electrode as the reference.

1.5 Calculation of CO Production and Selectivity

The CO production yield and gaseous product selectivity were calculated as follows:

$$V_{CO} = \frac{A_{CO}}{7103876.45361 \times 0.3} \times 16.8 \quad (1)$$

$$m_{CO} = \frac{V_{CO}}{22.4} \times 1000 \quad (2)$$

$$V_{CH_4} = \frac{A_{CH_4}}{6451887.01031 \times 0.3} \times 16.8 \quad (3)$$

$$m_{CH_4} = \frac{V_{CH_4}}{22.4} \times 1000 \quad (4)$$

$$V_{H_2} = \frac{A_{H_2}}{10882.94151 \times 0.3} \times 16.8 \quad (5)$$

$$m_{H_2} = \frac{V_{H_2}}{22.4} \times 1000 \quad (6)$$

where A_{CH_4}, A_{CO}, and A_{H_2} represent the chromatographic peak area of CH_4, CO, and

H_2 products, respectively. V_{CH_4}, V_{CO}, and V_{H_2} represent the volumes of CH_4, CO, and H_2 in reaction vessel, respectively. Correspondingly, m_{CH_4}, m_{CO}, and m_{H_2} denote their respective product yields (in μmol), which were calculated based on the measured gas concentrations and the total volume of the reaction system. *S* represents the percentage selectivity of each product.

$$S_{CO} = \frac{m_{CO}}{m_{co+}\ m_{CH_4} + m_{H_2}} \tag{7}$$

1.6 DFT calculations

All theoretical calculations were performed using the Vienna Ab Initio Simulation Package (VASP) within the framework of density functional theory (DFT).[1] The electron-ion interactions were described using the projector augmented wave (PAW) method,[2] and the Perdew–Burke–Ernzerhof (PBE) functional within the generalized gradient approximation (GGA) was employed to model exchange–correlation effects.[3] A kinetic energy cutoff of 550 eV was applied. Structural relaxations were considered converged when the total energy change was less than 1×10^{-4} eV and the maximum force on any atom was below 0.05 eV $Å^{-1}$.

A representative molecular fragment of the TTED-Hg-AF framework (denoted as the "MOF part") was extracted as the model. A 10 Å vacuum layer was introduced along all directions, and a 1 × 1 × 1 Monkhorst–Pack *k*-point mesh was used.

The adsorption energy (ΔE_{ads}) was calculated as

$$E_{ads} = E_{total} - E_{MOF\ part} - E_{adsorbate} \tag{8}$$

where E_{total}, $E_{MOF\ part}$, and $E_{adsorbate}$ represent the total energies of the adsorbate-substrate system, pristine TTED-Hg-AF fragment, and isolated CO_2 or H_2 molecule, respectively. A more negative ΔE_{ads} corresponds to stronger adsorption.

The CO_2 reduction pathway was modeled via four elementary steps:

1. CO_2 + MOF-part → MOF-part@CO_2
2. MOF-part@CO_2 + H → MOF-part@COOH
3. MOF-part@COOH + H → MOF-part@CO

4. MOF-part@CO → MOF-part + CO

The reaction energy change (ΔE) for each step is given by:

$$\Delta E = E_{products} - E_{reactants} \quad (9)$$

2. Supporting Figures

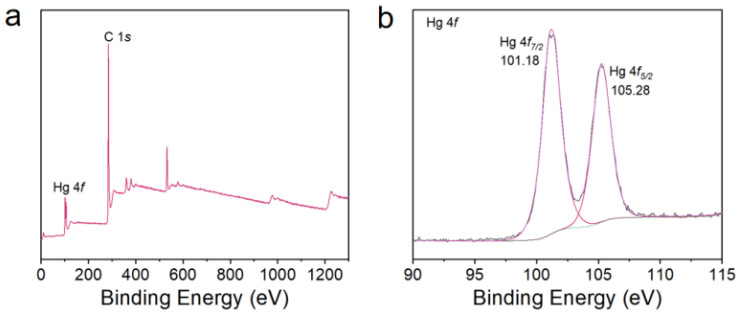

Figure S1. (a) XPS survey spectrum and (b) high-resolution Hg 4f XPS spectrum of TTED-Hg-AF.

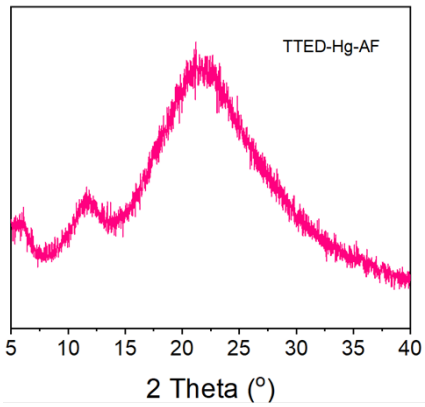

Figure S2. XRD pattern of TTED-Hg-AF.

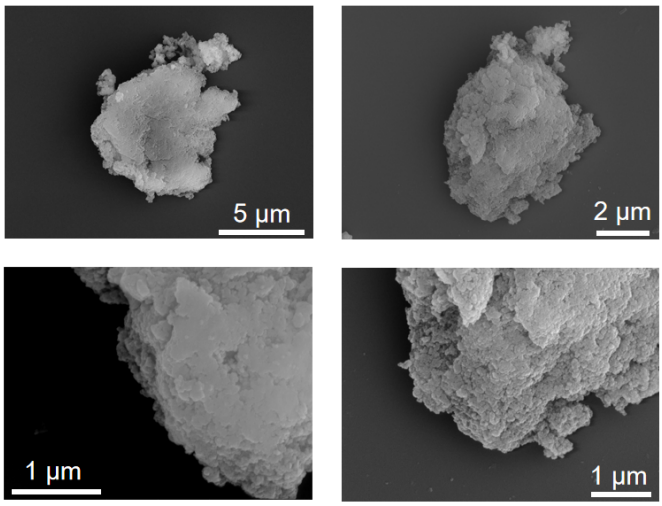

Figure S3. SEM images of TTED-Hg-AF nanosheets.

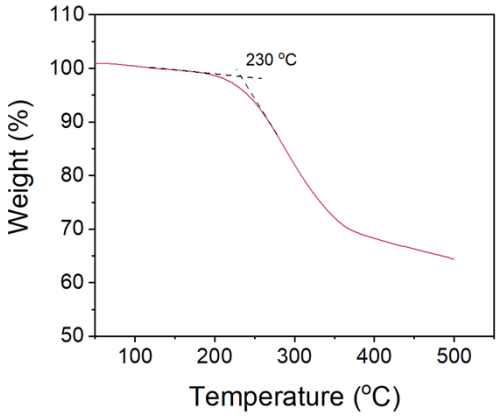

Figure S4. Thermogravimetric analysis (TGA) curve of TTED-Hg-AF.

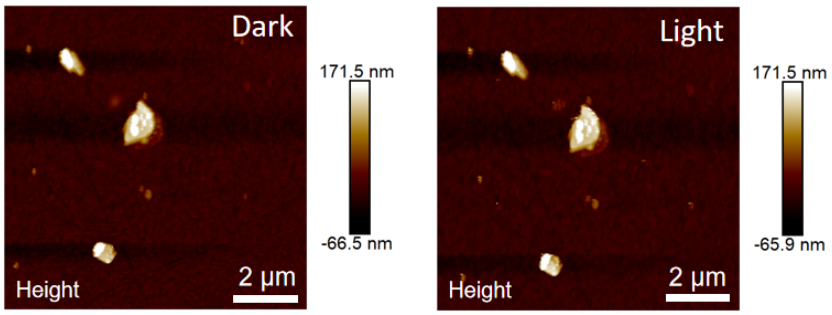

Figure S5. AFM height images of TTED-Hg-AF obtained during KPFM measurements (a) before and (b) after light irradiation.

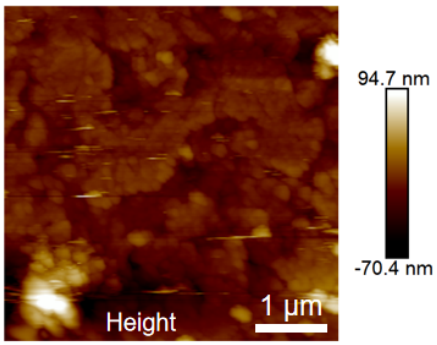

Figure S6. AFM height image of TTED-Hg-AF acquired during PFM measurements.

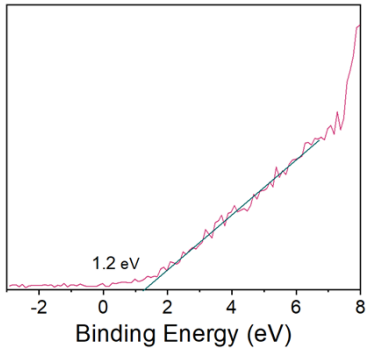

Figure S7. Valence band X-ray photoelectron spectroscopy (VB-XPS) spectrum of TTED-Hg-AF.

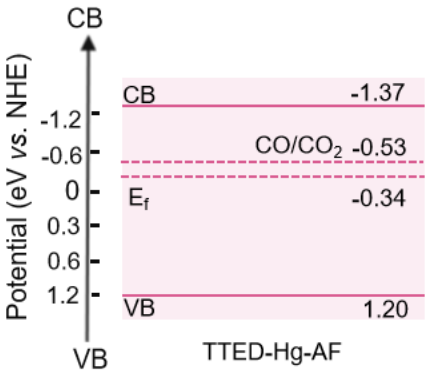

Figure S8. Schematic energy band structure diagram of TTED-Hg-AF determined from UV-vis DRS, Mott-Schottky, and VB-XPS measurements.

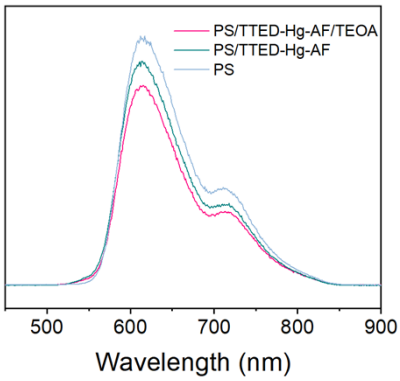

Figure S9. Photoluminescence (PL) spectra of $[Ru(bpy)_3]Cl_2$ photosensitizer (PS), PS/TTED-Hg-AF, and PS/TTED-Hg-AF/TEOA systems recorded under 400 nm excitation.

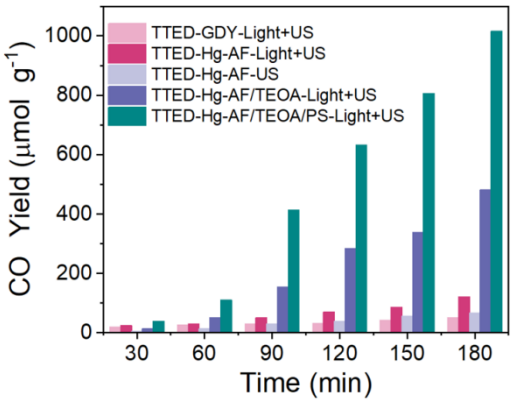

Figure S10. (a) Time-dependent CO production rates for various catalytic systems over 3 h of catalysis.

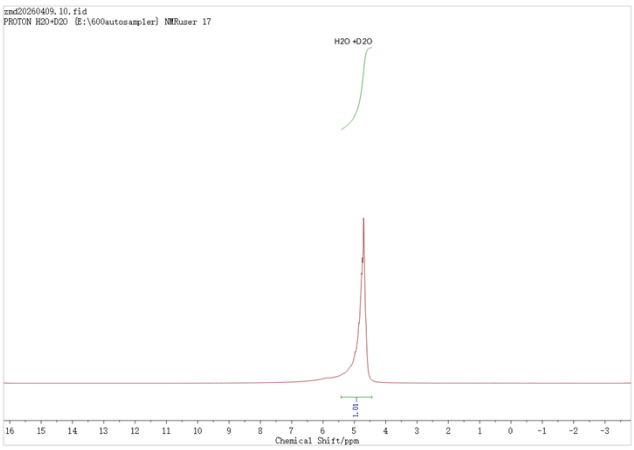

Figure S11. ^{1}H NMR spectrum of reacted liquid.

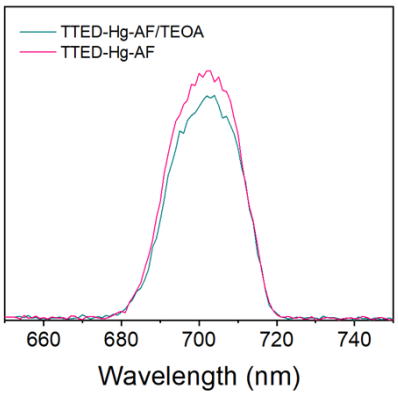

Figure S12. PL spectra of TTED-Hg-AF and TTED-Hg-AF/TEOA aqueous suspensions recorded under 350 nm excitation.

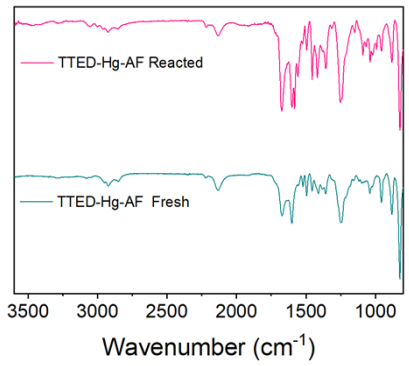

Figure S13. FTIR spectrum of TTED-Hg-AF before and after photocatalytic reaction.

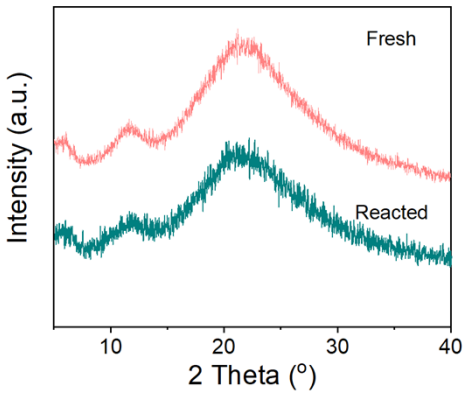

Figure S14. PXRD pattern of TTED-Hg-AF before and after photocatalytic reaction.

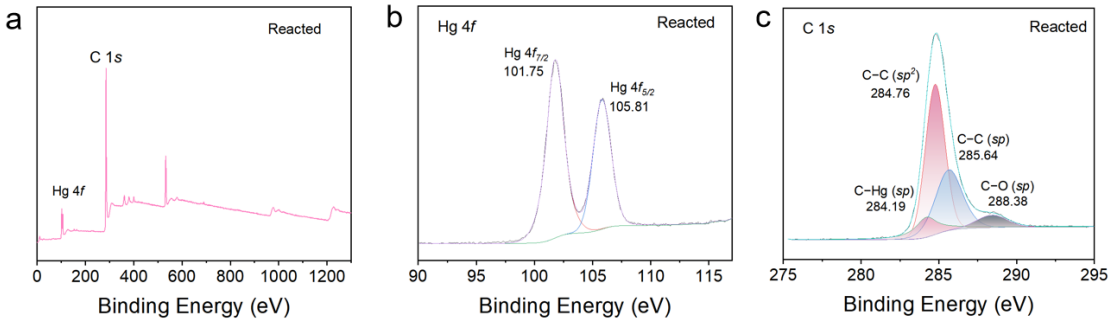

Figure S15. X-ray photoelectron spectroscopy (XPS) spectrum of TTED-Hg-AF after photocatalytic reaction.

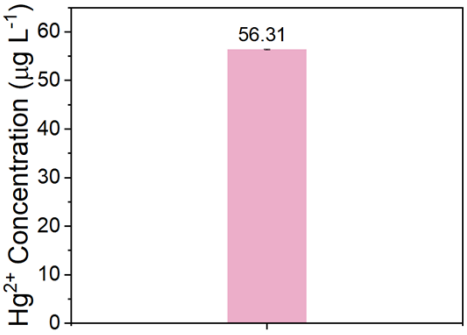

Figure S16. Hg^{2+} leaching concentration after reaction.

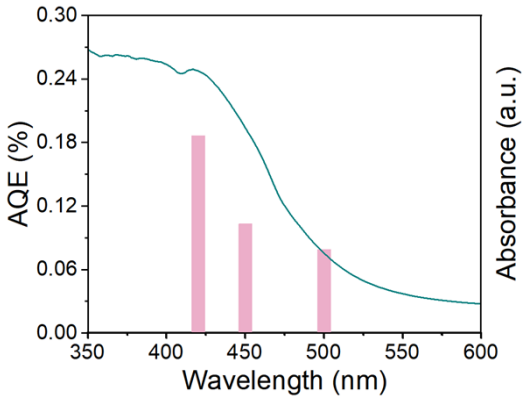

Figure S17. Apparent quantum efficiency (AQE) of TTED-Hg-AF powder measured at under 420, 450 and 500 nm wavelengths.

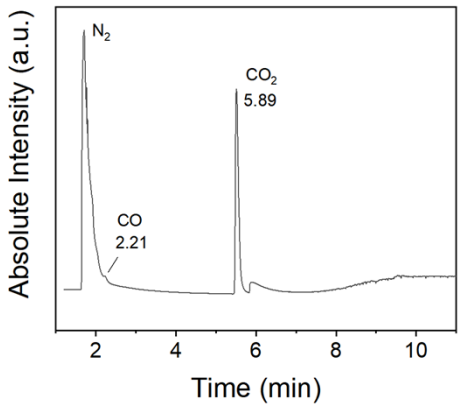

Figure S18. Total ion chromatographic (TIC) patterns for $^{13}CO_2$ catalytic reduction.

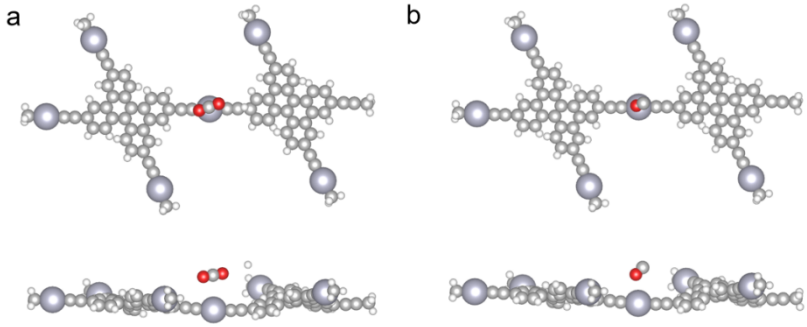

Figure S19. Optimized DFT geometries showing (a) *COOH and (b) *CO intermediates adsorbed on the TTED-Hg-AF surface.

3. References

1. G. Kresse and Furthmuller, Phys. *Rev. B: Condens. Matter Mater. Phys*., 1996, **54**, 11169.
2. G. Kresse and D. Joubert, *Phys. Rev. B: Condens. Matter Mater. Phys.*, 1999, **59**, 1758.
3. P. Perdew, K. Burke and M. Ernzerhof, *Phys. Rev. Lett*. 1996, **77**, 3865.